

Ultrafast X-Ray Phase-Contrast Imaging of the Initial Coalescence Phase of Two Water Droplets

Kamel Fezzaa[†] and Yujie Wang^{*}

X-ray Science Division, Argonne National Laboratory, 9700 South Cass Avenue, Argonne, Illinois 60439, USA
(Received 30 September 2007; published 13 March 2008)

We report an ultrafast x-ray phase-contrast imaging study of the early merging dynamics of two water drops in air. Owing to the edge-enhancement capability, the high penetrability, and the unprecedented temporal and spatial resolutions offered by this new x-ray technique, the coalescence singularity of two water drops was revisited. A finite initial contact radius was identified and the evolution of the trapped toroidal air bubble was studied for the first time. Despite the existence of this finite initial contact radius, the subsequent meniscus radius followed power laws which agree with theoretical predictions for the inviscid regime.

DOI: [10.1103/PhysRevLett.100.104501](https://doi.org/10.1103/PhysRevLett.100.104501)

PACS numbers: 47.20.Dr, 47.55.-t

When two liquid drops with small initial velocities make contact, they coalesce very rapidly. This seemingly simple free surface flow phenomenon has attracted both theoretical and experimental interests owing to its fundamental importance in fluid mechanics. It is a classical finite-time singularity problem [1–6] and the dynamics is governed by the nonlinear partial differential equations. Owing to the progress on both high-speed imaging and numerical simulation techniques, the understanding of hydrodynamic singularities has greatly advanced in recent years [7]. The dynamics close to the singularities are normally independent of the large-scale hydrodynamic behavior and controlled by simple scaling laws [7]. However, since the hydrodynamic fields at these singular points diverge, it poses great challenges for experimental studies due to their transient nature. One of the singularities which have attracted a lot of attention recently is the coalescence singularity. Despite the recent progress on both the theoretical and experimental fronts, there still exist many controversies. One of the major experimental discrepancies is whether the initial contact happens at a point or with a finite radius [5,6] and its influence on the subsequent dynamics. The determination of the dimensions of the tiny liquid bridge (meniscus) formed between the drops at the coalescence inception is essential to fit any scaling laws near the coalescence singularity. Uncertainty in the initial merging time has resulted in scaling laws with quite different exponents [5], which defeats any effort to further understand the nature of the initial contact. Furthermore, the complex interface profile close to the singularity as predicted by the theoretical studies [1,2] remains inaccessible to existing experimental techniques.

Here, we report the use of a new ultrafast x-ray full-field phase-contrast imaging technique, in order to reach some definite answers about the early stages of water drops coalescence. Deionized water was used in our experiment and a small amount of salt was added to provide the electrical trigger [3,5]. A pendent and a sessile drop were brought into contact to coalesce. The pendent drop has a radius of $953 \pm 5 \mu\text{m}$ and the sessile drop has a radius of

$1040 \pm 5 \mu\text{m}$. The drops' effective radius was $R = 995 \mu\text{m}$ [5]. Their approaching speed V_0 before contact was measured to be around 6.6 mm/s. The velocity is relatively high compared to previous studies in order to maintain repeatable coalescence events. The small effective impact Weber number of 4.8×10^{-3} indicates a soft coalescence regime characterized by small droplet deformation [8].

The high spatial and temporal resolutions required for this experiment were made possible by the intense white x-ray beam (full energy spectrum) delivered by the XOR 32-ID undulator beam line of the Advanced Photon Source of Argonne National Laboratory, which has a peak irradiance of 10^{14} ph/s/mm²/0.1%bw. The time structure of the filling pattern (hybrid mode) in the storage ring is such that there is an x-ray pulse 472 ns long every 3.6 μs [9], which we used to expose each image. Thus, this unprecedented time resolution (472 ns) is achieved by using the natural width of the x-ray pulses. Our detector consisted of a fast LYSO:Ce scintillator (LYSO denotes lutetium yttrium oxyorthosilicate) coupled to a high-efficiency CCD camera (Sensicam, Cooke Corp., 1024×1280 pixels) via a microscope objective (5x, with a numerical aperture of 0.14). The detector was synchronized and gated to the x-ray pulses. The coalescence setup was located about 170 mm upstream of the detector. This corresponded to an optimized defocus value for Fresnel propagation contrast and effective spatial resolution. The drops were brought together by siphoning effect from a water tank. The location of the large free water surface above the contact point allowed precise control of the coalescence event frequency and repeatability. Using the electrical trigger from the drops as a reference, a series of logic electronics and delay generators was used to probe the coalescence event from inception to fully merge in a stroboscopic mode. For each time delay, many images (from different events) were taken to check the measurement reliability. This ensemble average technique is justified by the small variations in the meniscus radii and heights obtained at fixed delay time. The detector system

has a $2.4 \mu\text{m}$ spatial resolution [full width at half maximum (FWHM) of the measured point spread function (PSF)]. This spatial resolution offers us the capability to detect small sized features ($\sim 5 \mu\text{m}$) such as air bubble and particles which has been demonstrated in our recent publication [10].

X-ray phase-contrast imaging mainly enhances sharp boundaries and interfaces between materials with different refraction indices or abrupt thickness variations [11]. This unique capability is particularly suitable for the current application where we are mostly interested in the air-water interfaces. Figure 1 shows the early merging profiles of the two water drops as captured with x rays. Unlike in visible-light imaging, the image contrast is most significant at the air-water interfaces which lead to straightforward image interpretation. In the edge-enhancement regime, each boundary is signified as a pair of black and white fringes due to the partial coherent nature of the white x-ray beam. The image contrast can be treated as a simple x-ray refraction effect by the highly curved air-water interfaces [11]. The relatively high x-ray energy ($\sim 13 \text{ keV}$) utilized in the current experiment ensured that the image contrast was mostly dominated by phase-contrast instead of absorption-contrast. Thus, quite uniform intensity is observed in the body of the drops despite its sheer thickness along the x-ray path. Phase contrast is naturally immune to the strong reflection or scattering effects that are usually associated with visible-light imaging. These strong reflection or scattering effects can lead to difficulty in image interpretation. The close-up details of the very early profiles of the coalescence process are shown in Fig. 2. The air-water interface at the meniscus forms a complex lens system that

refracts (deviates) x rays from their original path, resulting in a focusing effect. Each bright feature can be paired with a dark feature from which x rays were deviated. This effect is clearly visible at the four corners of the meniscus. The smallest meniscus height which can be resolved in the current experiment was around $5 \mu\text{m}$. It turns out that the measurement of this dimension was crucial to the unambiguous determination of the start of the coalescence process. The complex internal structure of the meniscus was also visible owing to the high penetrability of the x rays. It was observed recently that there exists a 90° corner at the air-water interface when two water drops coalesce while the interface for water-glycerol mixture is much more gradual [4]. It is clear from Fig. 2 that this 90° corner is actually a curved-in toroidal bubble suggested by Eggers *et al.* [1] even though the original work was mostly focused on the viscous regime. It was theoretically predicted that the merging dynamics is very different depending on whether there exists an external viscous fluid [12,13]: whenever there exists an outer fluid, no matter how small its viscosity is, there would always be a bubble-like structure formed at the contact point. It originates from the fact that due to the rapidity of the merging, only part of outer fluid trapped between the water spheres can escape, the rest accumulates into a toroidal bubble which connects to the outer neck. As suggested by Eggers *et al.* [1], the toroidal bubble and the neck would follow different dynamics, which, as a result, will lead to the eventual escape of the bubble at the end of the coalescence. However, due to the concave shape of the toroidal bubble formed, it was not observed until the current study. In Fig. 2, the curved-in bubblelike structure is clearly visible in all images until

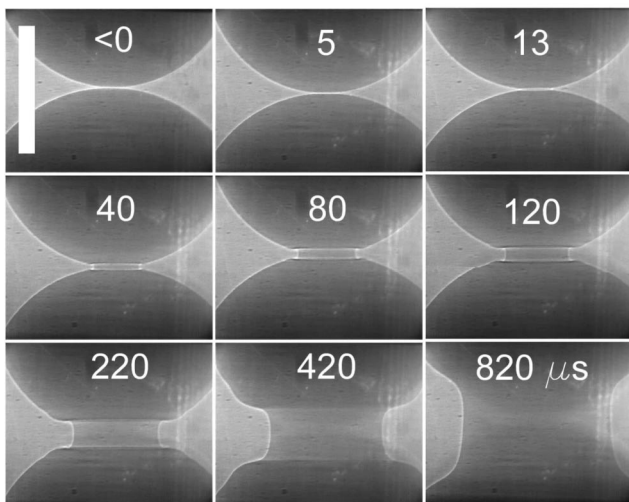


FIG. 1. Water drops coalescence process recorded with ultrafast high-resolution x-ray phase-contrast imaging with 472 ns exposure time. The images give an overview of the two drops with enhanced boundaries through the phase-contrast mechanism. The scale bar is 1 mm long. The numbers indicate the time instances relative to the start of merging (SOM).

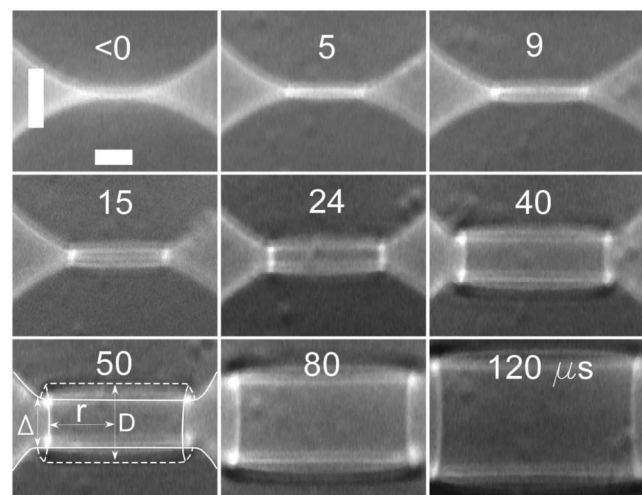


FIG. 2. Close-up views of the contact region show the liquid bridges (meniscus) in the early stage of the merging. Notice the different vertical and horizontal scale bars. The vertical and horizontal scale bars are 50 and $100 \mu\text{m}$ long, respectively. The highly concave air-water interfaces with trapped toroidal air bubbles are visible as indicated by the guide.

400 μs after the start of the coalescence as shown in Fig. 1 suggesting that the bubble has finally escaped.

One of the critical questions faced by the hydrodynamic singularity study is the determination of its inception time since any subsequent scaling study is dependent upon it. It was suggested that a slight misalignment of the axes of the drops could result in an uncertainty of the starting point of the coalescence in visible-light imaging. Instead, the line-of-sight nature of x-ray imaging makes it easy to distinguish between an overlap due to misalignment [Fig. 3(a)] and an actual merging [Fig. 3(b)]. The difference between the images formed for two scenarios is clearly visible and is due to their respective thickness gradient profiles along the x-ray path. Figures 3(c) and 3(d) are the corresponding Fresnel diffraction simulations.

The smallest meniscus gap width Δ we can resolve was around 5 μm . It follows a linear curve up to ~ 0.4 ms with a speed of 0.90 ± 0.01 m/s as shown in Fig. 4. This linear law is a natural confirmation of the theoretical prediction that $\Delta \sim r^2$ [1], where r is the meniscus radius in the inertial regime. The time zero of the coalescence can thus be determined by extrapolating the linear curve back to intercept the time axis [1]. It turns out to be 5 ± 0.15 μs before our earliest image and about 10 μs after the electrical trigger.

By using a scaling argument, it was predicted [1,2] that the meniscus radius r grows with time by a power law when the coalescence is dominated by inertia: $r \sim (\sigma R/\rho)^{1/4} t^{1/2}$, where σ , ρ , and R are the surface tension, density and droplet radius respectively [4–6]. With the exact coalescence time determined in our case, the radius of the meniscus can be fitted with a power law of

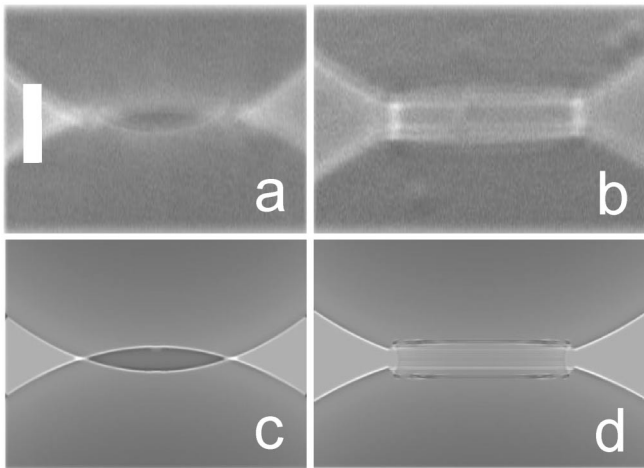


FIG. 3. Phase-contrast imaging contrast comparison of drops when they are merging or simply spatially overlapping. Panel (a) and (c) shows the experimental and simulation images when the drops are spatially overlapping and panel (b) and (d) show the corresponding merging case. The image contrast between two scenarios is clearly different, which is crucial for the determination of the coalescence time. The scale bar is 50 μm long.

the form $r(\mu\text{m}) = r_0 + a[t(\mu\text{s})^b]$ (Fig. 4). The resulting fitting parameters are $r_0 = 43.8 \pm 4.3$, $a = 18.1 \pm 1.9$, and $b = 0.50 \pm 0.02$. Thus, a finite initial contact radius is unambiguously identified. Additionally, despite the finite initial contact radius, the subsequent dynamics still follow the power law scaling relationship which is in good agreement with the theoretical predictions [1,2]. Furthermore, the scaling relationship can be rewritten in dimensionless form, in which the spatial and temporal dimensions are normalized by R and $\sqrt{\rho R^3/\sigma}$, respectively: $r = 0.05 + 1.10t^{0.50}$, also in good agreement with previously reported results [4,6].

The toroidal bubble height D also follows a power law scaling relationship $D(\mu\text{m}) = c[t(\mu\text{s})^d]$. The resulting fitting parameters are $c = 2.29 \pm 0.2$, and $d = 0.85 \pm 0.02$. The scaling law exponent was obtained for the first time in the inertial regime [1,2]. The resulting dimensionless scaling law is $D = 2.43t^{0.85}$.

The error bars associated with the data points in Fig. 4 are of the order of the symbol sizes we used. They are mainly caused by the strobe nature of the experiment and not by the temporal and spatial resolutions of the experimental setup which we estimate to be within 2 μs and 2.4 μm , respectively.

Quasistatic merging is a particular case of a more general problem of droplets collision for which a comprehensive theory has been developed recently [8,14]. Theoretical studies predicted that the droplets undergo a deformation just before merging due to the buildup of air pressure in between, and subsequently form a flattened disk shape

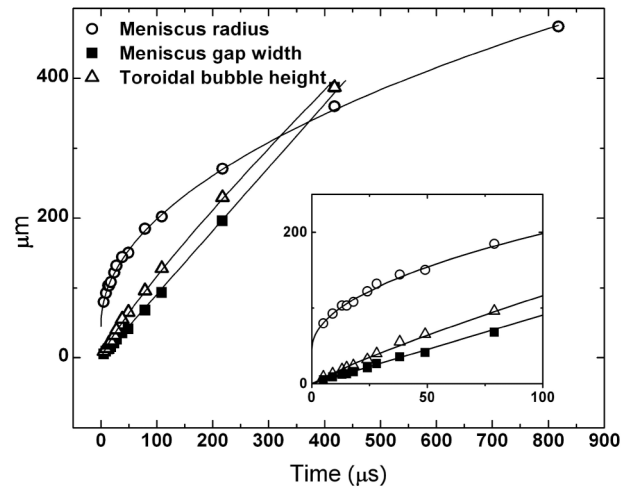


FIG. 4. Meniscus radius, meniscus gap width, and the toroidal bubble height as a function of time. Symbols are experimental data and the lines are power laws fittings. The inset shows data close to the coalescence onset. The meniscus gap width and toroidal bubble height were extracted only up to 0.4 ms due to the ambiguity of their definitions when the bubble escaped. The error bars for both temporal and spatial measurement are about the sizes of the symbols in the inset.

interface with a radius $r_0 = (3\mu_{\text{air}}V/2\sigma)^{1/4}R$ in the constant approaching velocity scenario [8], where μ_{air} is air viscosity. This initial radius shows a weak dependence on the approaching velocity and predicts a value of $r_0 = 40.2 \mu\text{m}$ which coincides with the finite initial contact radius identified in our measurement. However, despite the fact we can identify this initial contact radius, the exact nature of the coalescence moment is still beyond current work.

Indeed, for the merging to happen, the gap between the two liquid surfaces must be small enough for van der Waals attractive molecular forces to become effective and rupture the interfaces. This critical value is typically a few hundred angstroms [8].

Depending on the experimental parameters, the contact interface most likely form a dimple and the minimal gap would be located along its perimeter, so the merging will happen through a rupture at the boundary by entrapping an air bubble [8]. Even if this is not the case, it was suggested by Duchemin *et al.* [2] that a center rupture scenario will lead to the excitations of the capillary waves at the very early stages of the coalescence which can cause repeated connections of the gap to form small air bubbles. Thus, in both scenarios, there will be microscopic air bubbles formed. However, the latter scenario will lead to wrong scaling relationship which will disagree with current study.

Direct observation to differentiate these two scenarios is beyond our present experimental capability, since it requires us to differentiate micron-sized air bubbles. We can infer the size of the air bubbles indirectly with the following argument. A rupture around the disk rim would entrap the intervening gas and form a bubble inside the merging droplets. The smallest air bubble can be detected in the current setup is $5 \mu\text{m}$. Using $r_0 = 43.8 \mu\text{m}$, assuming an initial air disk thickness $h(0)$ of about 100 \AA , the air bubbles formed will be very close to our spatial resolution.

In conclusion, the early merging dynamics has been revisited and the internal toroidal bubble evolution studied for the first time by the x-ray ultrafast phase-contrast imaging technique. Because of the combined order of magnitude improvement in time and spatial resolution, and the sensitivity of this method, we demonstrated that the early stages of the coalescence can unambiguously be observed to verify theory. The intricate physics behind

the molecular nature of merging is still an open field, both theoretically and experimentally. This new technique will be an invaluable tool to improve our understanding of the finite-time hydrodynamic singularities in which the self-similar interface profiles and dynamic scaling laws carry most of the underlying physics. This is particularly important when visible-light imaging suffers from strong refraction, reflection, or scattering effects close to small spatial dimensions or simply cannot be used for optically opaque systems.

The authors would like to thank C. K. Law, I. McNulty, and H. A. Stone for the insightful discussions. The use of the APS was supported by the U.S. Department of Energy, Office of Science, Office of Basic Energy Sciences, under Contract No. DE-AC02-06CH11357 and Argonne National Laboratory Director's Competitive Grant (LDRD) No. 2006-023-R1.

*yujie@aps.anl.gov

†fezzaa@aps.anl.gov

- [1] J. Eggers, J. R. Lister, and H. A. Stone, *J. Fluid Mech.* **401**, 293 (1999).
- [2] L. Duchemin, J. Eggers, and C. Josserand, *J. Fluid Mech.* **487**, 167 (2003).
- [3] A. Menchaca-Rocha *et al.*, *Phys. Rev. E* **63**, 046309 (2001).
- [4] M. M. Wu, T. Cubaud, and C. M. Ho, *Phys. Fluids* **16**, L51 (2004).
- [5] S. T. Thoroddsen, K. Takehara, and T. G. Etoh, *J. Fluid Mech.* **527**, 85 (2005).
- [6] D. G. Aarts *et al.*, *Phys. Rev. Lett.* **95**, 164503 (2005).
- [7] J. Eggers, *Rev. Mod. Phys.* **69**, 865 (1997).
- [8] P. Zhang and C. K. Law, *Proceedings of the 5th U.S. National Combustion Meeting, Western States Section/Combustion Institute (WSS/CI), San Diego, CA, March 25-28*, Paper No. G16, 2007.
- [9] http://aps.anl.gov/Facility/Storage_Ring_Parameters/.
- [10] K.-S. Im *et al.*, *Appl. Phys. Lett.* **90**, 091919 (2007).
- [11] S. W. Wilkins *et al.*, *Nature (London)* **384**, 335 (1996).
- [12] J. B. Keller and M. J. Miksis, *SIAM J. Appl. Math.* **43**, 268 (1983).
- [13] R. W. Hopper, *J. Am. Ceram. Soc.* **76**, 2953 (1993).
- [14] M. A. Rother, A. Z. Zinchenko, and R. H. Davis, *J. Fluid Mech.* **346**, 117 (1997).